Liquid-gas phase transition of thermal nuclear matter and the in-medium balance between nuclear attraction and repulsion

Shen Yang (杨申),[1] Xiang Dong Sun (孙向东),[1] Jing Geng (耿晶),[1] Bao Yuan Sun (孙保元),[1,*] and Wen Hui Long (龙文辉)[1,2,3,†]

[1]*School of Nuclear Science and Technology, Lanzhou University, Lanzhou 730000, China*
[2]*Joint Department for Nuclear Physics, Lanzhou University and Institute of Modern Physics, CAS, Lanzhou 730000, China*
[3]*Key Laboratory of Special Function Materials and Structure Design, Ministry of Education, Lanzhou 730000, China*

(Received 15 June 2020; revised 15 November 2020; accepted 22 December 2020; published 8 January 2021)

Properties of the liquid-gas (LG) phase transition of thermal nuclear matter are investigated within the relativistic Hartree-Fock (RHF) theory, focusing on the role played by the in-medium balance between nuclear attraction and repulsion. Applying the RHF Lagrangian PKA1, rather different critical properties and LG phase diagrams are obtained in contrast to the other popular relativistic Lagrangians. Aiming at such notable model deviations, a series of testing parametrizations $x\kappa_\rho$ (κ_ρ being the ρ-tensor coupling strength) are proposed to bridge PKA1 and other popular Lagrangians. Along the systematics from PKA1 to the $x\kappa_\rho$ series and further to other popular Lagrangians, it is illustrated that the in-medium balance of nuclear attraction and repulsion, manifested as various modeling of the nuclear in-medium effects, is essential for the van der Waals-like behaviors of thermal nuclear matter, in which the residual nuclear in-medium effects deduced from the dominant attractive and repulsive channels play a significant role. Our study paves a way to model the in-medium nuclear interactions from the thermal statistic aspects of nuclear systems, e.g., referring to the critical temperature from future delicate experiments.

DOI: 10.1103/PhysRevC.103.014304

I. INTRODUCTION

Features of nuclear matter at finite temperature are of fundamental significance in nuclear physics. Due to the van der Waals-like behavior of nucleon-nucleon interaction, namely the natures of short-range repulsion and medium-long-range attraction of nuclear force, the so-called liquid-gas (LG) phase transition similar to that in condensed matter can occur in subsaturated thermal nuclear matter [1,2]. In experiments, the LG phase transition is explored from the survey of the nuclear caloric curve and multifragment distribution in heavy-ion collisions [3–9]. The LG phase transition of thermal nuclear matter has been studied both experimentally and theoretically over the past decades [3–22], and its important impact has aroused extensive attention from the community in areas such as heavy-ion collisions [17,18,20,21], nuclear astrophysics [23–27], etc.

The LG phase transition can occur in symmetric and asymmetric nuclear matter. In symmetric nuclear matter, lots of effort has been devoted to the critical parameters of the LG phase transition, particularly for the critical temperature T_C. In general, T_C is predicted as 10–20 MeV by various nuclear models [2,12,13,28–32], showing notable uncertainty. In fact, it is also very hard to deduce a precise T_C value from the experimental side [4,5,9,16]. However, the correlations between T_C and other LG critical parameters, such as critical pressure P_C, or other bulk quantities of nuclear matter can help us to reduce the uncertainty [33]. In asymmetric nuclear matter, the isospin dependence of the properties of the LG phase transition has attracted much attention of the experimentalists in recent years [7,8,34,35]. Theoretically, a phase diagram structure in a wide range of isospin asymmetry and pressure is predicted for the LG phase transition [13,30,36–40]. The relation between the LG phase diagram properties and the equation of state of nuclear matter, especially the symmetry energy, has been studied intensively [13,30,38,41], but is missing a quantitative interpretation from the aspect of nuclear force.

As one of the popular nuclear models, the relativistic mean-field (RMF) theory that contains only the Hartree terms of the meson-nucleon couplings, also referred to as the covariant density functional theory (CDFT), has been used to great success in describing the properties of finite nuclear and nuclear matter [42–50]. To provide accurate descriptions of nuclear properties, such as the appropriate incompressibility of nuclear matter [43], the nuclear in-medium effects have been introduced on the level of the RMF approach, by collaborating with either the nonlinear self-couplings of mesons or the density dependencies of the meson-nucleon coupling strengths [51–57]. Practically, the RMF models have been widely applied to study the LG phase transition of thermal nuclear matter [13,37–39,58]. For instance, the critical temperature T_C was predicted by the RMF calculations around 15 MeV [13,37–39,58], still showing certain model dependence. For the behaviors of the LG phase diagram, it is suggested by the RMF models that the size of the LG phase coexistence

*sunby@lzu.edu.cn
†longwh@lzu.edu.cn

 ©2021 American Physical Society

area may be dominated by the slope of the symmetry energy [13,37–39].

Almost in parallel with the development of the RMF theory, there also exist some attempts on the relativistic Hartree-Fock (RHF) descriptions of finite nuclei and nuclear matter [59–62], whereas the quantitative accuracy of the RHF calculations is not comparable with the conventional RMF models at that moment. Until considering the density dependencies of the meson-nucleon coupling strengths, namely the density-dependent relativistic Hartree-Fock (DDRHF) theory [63–66], accuracy similar to that of the RMF models was achieved on describing the nuclear structure and nuclear matter properties with the proposed RHF Lagrangians PKOi ($i=$ 1, 2, and 3) [63,65] and PKA1 [64], and a series of significant improvements was also found with the presence of the Fock terms [67–80]. Notice that the nuclear in-medium effects have been evaluated phenomenologically by using the density dependencies of the meson-nucleon coupling strengths in DDRHF [63,64].

Recently it has been revealed in Ref. [81] that because of the ρ-tensor (ρ-T) coupling, which contributes a fairly strong attractive potential, the in-medium balance between the nuclear attraction and repulsion carried by the σ-scalar (σ-S) and ω-vector (ω-V) couplings is notably changed in PKA1, compared to the other RMF and RHF Lagrangians. As a result, it brings notable improvement upon the restoration of the pseudo-spin symmetry (PSS) [82–88] of the high-l pseudo-spin (PS) partners, and the spurious shell closures found commonly in the RMF calculations and the RHF ones with PKOi [64,81,89] are eliminated. In fact, the RHF models with PKOi have also been applied in studying the LG phase transition of thermal nuclear matter [33] and predict similar LG phase transition properties as the popular RMF models. Considering the ρ-T coupling, namely PKA1, we find in this work that the predicted LG phase transition properties become notably different. In analogy to the restoration of the PSS in finite nuclei, it inspires us to investigate the physics that is essentially related to the LG phase transition of thermal nuclear matter, particularly for the role of the ρ-T coupling.

In this work, which employs the finite-temperature RMF and RHF models, the critical parameters and phase diagrams of the LG phase transition of thermal nuclear matter are studied in detail by focusing on the role of ρ-T coupling and the deduced effects. The paper is organized as follows. The formalism of the RHF theory for thermal nuclear matter is briefly introduced in Sec. II. In Sec. III we present the calculated results and discussions, including the general properties of the LG phase transition in Sec. III A and in Sec. III B the role played by the ρ-T coupling, as well as the deduced effects. Finally, a short summary is given in Sec. IV.

II. RHF FORMALISM FOR THERMAL NUCLEAR MATTER

Based on the meson exchange picture of nuclear force, the Lagrangian density, a starting point of the RHF theory, can be constructed by considering the degrees of freedom associated with nucleons (ψ), two isoscalar mesons (σ and ω), two isovector mesons (π and ρ), and photons (A). For uniform nuclear matter systems, the photon field A, which describes the electromagnetic interactions between charged particles, is ignored in this work. Thus, the Lagrangian density can be expressed as

$$\mathscr{L}_0 = \mathscr{L}_M + \mathscr{L}_\sigma + \mathscr{L}_\omega + \mathscr{L}_\rho + \mathscr{L}_\pi + \mathscr{L}_I, \tag{1}$$

where the Lagrangians $\mathscr{L}_\phi$ ($\phi = \psi, \sigma, \omega^\mu, \vec{\rho}^\mu$, and $\vec{\pi}$) represent the free nucleon (ψ) and meson ($\sigma, \omega^\mu, \vec{\rho}^\mu$, and $\vec{\pi}$) fields,

$$\mathscr{L}_M = \bar{\psi}(i\gamma^\mu\partial_\mu - M)\psi, \tag{2}$$

$$\mathscr{L}_\sigma = +\tfrac{1}{2}\partial^\mu\sigma\partial_\mu\sigma - \tfrac{1}{2}m_\sigma^2\sigma^2, \tag{3}$$

$$\mathscr{L}_\omega = -\tfrac{1}{4}\Omega^{\mu\nu}\Omega_{\mu\nu} + \tfrac{1}{2}m_\omega^2\omega_\mu\omega^\mu, \tag{4}$$

$$\mathscr{L}_\rho = -\tfrac{1}{4}\vec{R}_{\mu\nu}\cdot\vec{R}^{\mu\nu} + \tfrac{1}{2}m_\rho^2\vec{\rho}^\mu\cdot\vec{\rho}_\mu, \tag{5}$$

$$\mathscr{L}_\pi = +\tfrac{1}{2}\partial_\mu\vec{\pi}\cdot\partial^\mu\vec{\pi} - \tfrac{1}{2}m_\pi^2\vec{\pi}\cdot\vec{\pi}, \tag{6}$$

with the field tensors $\Omega^{\mu\nu} \equiv \partial^\mu\omega^\nu - \partial^\nu\omega^\mu$, $\vec{R}^{\mu\nu} \equiv \partial^\mu\vec{\rho}^\nu - \partial^\nu\vec{\rho}^\mu$, and $F^{\mu\nu} \equiv \partial^\mu A^\nu - \partial^\nu A^\mu$. Incorporating with the Lorentz scalar (σ-S), vector (ω-V and ρ-V), tensor (ρ-T), and pseudo-vector (π-PV) couplings, the Lagrangian $\mathscr{L}_I$, which describes the interactions between nucleons and mesons, reads as

$$\mathscr{L}_I = \bar{\psi}\bigg(- g_\sigma\sigma - g_\omega\gamma^\mu\omega_\mu - g_\rho\gamma^\mu\vec{\tau}\cdot\vec{\rho}_\mu + \frac{f_\rho}{2M}\sigma_{\mu\nu}\partial^\nu\vec{\rho}^\mu\cdot\vec{\tau} - \frac{f_\pi}{m_\pi}\gamma_5\gamma^\mu\partial_\mu\vec{\pi}\cdot\vec{\tau}\bigg)\psi. \tag{7}$$

In the above Lagrangian densities, M and m_ϕ denote the masses of nucleons and mesons, and g_ϕ ($\phi = \sigma$-S, ω-V, ρ-V) and $f_{\phi'}$ ($\phi' = \pi$-PV, ρ-T) represent relevant meson-nucleon coupling strengths. Here we use arrows for isovectors.

Notice that in the RHF Lagrangian PKO2 [65], only the σ-S, ω-V, and ρ-V couplings are considered, and further in PKOi ($i = 1$ and 3) [63,65] the π-PV coupling that contributes only via the Fock terms is taken into account. In this work, we focus on the RHF calculations with PKA1 [64], which is further implemented by the degree of freedom of the ρ-T coupling that plays the role almost fully via the Fock terms. To provide accurate descriptions of nuclear matter and finite nuclei, the meson-nucleon coupling strengths g_ϕ and $f_{\phi'}$ are assumed to be functions of the nucleon density ρ_b to evaluate the nuclear in-medium effects, and the details can be found in Refs. [63,64].

From the Lagrangian density (1), one can get the Hamiltonian density $\mathscr{H}$ via the Legendre transformation. Following the standard procedure in Ref. [60], the energy functional E, namely the energy density of nuclear matter, can be obtained by taking the expectation of the Hamiltonian $\mathscr{H}$ with respect to the Hartree-Fock ground state $|\Phi_0\rangle$ [60,77],

$$E \equiv \langle\Phi_0|\mathscr{H}|\Phi_0\rangle = E^{\text{kin}} + \sum_\phi \big(E_\phi^D + E_\phi^E\big), \tag{8}$$

where E^{kin}, E^D, and E^E correspond to the kinetic, the Hartree, and the Fock potential energies, respectively, and $\phi = \sigma$-S, ω-V, ρ-V, ρ-VT (the ρ-vector-tensor coupling), ρ-T, and π-PV (ρ-VT for the ρ-vector-tensor coupling). For further details, please refer to Refs. [33,77].

In this work, we devote ourselves to the LG phase transition of thermal nuclear matter. To take the effects of finite temperature into account, we introduce the grand canonical ensemble in quantum statistical mechanics, in which the thermal equilibrium for a statistical N-body system can be deduced from the variation of the grand canonical potential Ω,

$$\Omega = F - \mu N = E - TS - \mu N. \tag{9}$$

In the grand canonical potential Ω, F, E, T, S, and μ are the free energy, the total energy, the temperature, the entropy and the chemical potential of thermal nuclear matter, respectively.

Since nuclear matter is a fermionic system, the Fermi-Dirac distribution $n_\tau(p)$ is introduced for thermal nuclear matter as

$$n_\tau(p) = \frac{1}{1 + \exp[(\varepsilon(p,\tau) - \mu_\tau)/T]}, \tag{10}$$

where $\varepsilon(p,\tau)$ is the single-particle energy of the state $i = (p, s, \tau)$, and p, s, and τ correspond to the momentum and the spin and isospin projections, respectively. Here we appoint $\tau = 1$ and -1 for neutron and proton, respectively. For further details, the readers are referred to Ref. [33]. In the following, we just briefly recall the quantities of the LG phase transition which we focus on.

To study the LG phase transition of thermal nuclear matter, particularly the coexistence of the liquid (L) and gas (G) phases, one needs to solve the phase coexistence equations, namely the Gibbs conditions,

$$\mu_\tau^L(T, \rho_b^L, \delta^L) = \mu_\tau^G(T, \rho_b^G, \delta^G), \tag{11a}$$

$$P^L(T, \rho_b^L, \delta^L) = P^G(T, \rho_b^G, \delta^G), \tag{11b}$$

where ρ_b is the nucleon density and δ represents the isospin asymmetry, i.e., $\delta = (N - Z)/(N + Z)$. The pressure P of thermal nuclear matter can be obtained from the thermodynamic relation as

$$P = \rho_b^2 \frac{\partial}{\partial \rho_b} \frac{F}{\rho_b} = TS + \sum_{i=n,p} \mu_i \rho_i - E(\rho_b, \delta, T). \tag{12}$$

For symmetric nuclear matter, the critical point, namely the inflection point of the pressure curve with respect to the nucleon density ρ_b, can be determined by the following condition,

$$\left.\frac{\partial P}{\partial \rho_b}\right|_{T=T_C} = \left.\frac{\partial^2 P}{\partial \rho_b^2}\right|_{T=T_C} = 0, \tag{13}$$

from which one can extract the critical parameters, such as the critical temperature T_C, the critical density ρ_C, the critical pressure P_C, etc. It is worthwhile to mention that there exists a linear relationship among the P_C, the ρ_C, and the critical incompressibility K_C [33]:

$$K_C + 18\frac{P_C}{\rho_C} = 0, \quad K_C \equiv 9\rho_b^2 \frac{\partial^2}{\partial \rho_b^2} \left.\frac{F}{\rho_b}\right|_{\rho_b=\rho_C}. \tag{14}$$

In fact, people often introduce the compressibility factor $Z_C \equiv P_C/\rho_c T_C$. Thus, K_C and Z_C provide a concise way to understand the critical point of the LG phase transition of symmetric nuclear matter.

III. RESULTS AND DISCUSSION

In this work, special emphasis is paid to the role of the ρ-T coupling in determining the LG phase transition of thermal nuclear matter. The calculations are carried out by using the DDRHF models, as compared to the RMF models with the nonlinear self-coupling of mesons and the density-dependent meson-nucleon coupling strengths (DDRMF). In thermal nuclear matter, with the introduction of the Fermi-Dirac distribution, the momentum integration from zero to the Fermi momentum p_F is replaced by the momentum integration from zero to the infinite. Practically, it is performed by the Gauss-Legendre integral formalism with a momentum cutoff of $p = 5p_F$ after careful numerical test. Specifically, the phase coexistence equations (11) regarded as a set of nonlinear equations are solved by the Powell hybrid method [90] (see Ref. [33] for details).

A. LG phase transition described by PKA1

In this subsection, we focus on the critical parameters and phase diagrams of the LG phase transition described by the RHF Lagrangian PKA1. Because of the presence of the ρ-T coupling in PKA1, the predicted properties of the LG phase transition of thermal nuclear matter can be largely different from the RMF calculations and the RHF calculations with PKO*i* [33], as we will see.

Utilizing PKA1, Fig. 1 shows the pressure P (MeV fm^{-3}) of symmetric nuclear matter as a function of density ρ_b (fm^{-3}) at various temperatures. It can be seen that the pressure curves given by PKA1 show the typical behavior of the S shape of the van der Waals-like isotherm [2,11,29,31,32,91,92], being consistent with the other relativistic calculations [33]. From the critical point in Fig. 1, we extracted the critical parameters of the LG phase transition of symmetric thermal nuclear matter, namely the critical temperature T_C, density ρ_C, pressure P_C, incompressibility K_C, and impressibility factor Z_C. The results are shown in Table I, as compared to the results given by the RHF Lagrangian PKO3 [65] and the RMF Lagrangians DD-ME2 [93] and PK1 [53].

Obviously, the T_C value given by PKA1 is evidently smaller than the ones given by the other selected Lagrangians. In fact, the popular RMF and RHF Lagrangians predict T_C = 13–18 MeV [33], values which are systematically larger than the prediction of PKA1. Except for ρ_C, there also exist notable differences in the other critical parameters between PKA1 and the other Lagrangians. As the combination of P_C, ρ_C, and T_C, the Z_C value given by PKA1 reads as 0.196, which also deviates notably from the values given by the other Lagrangians [33]. All these indicate that the van der Waals-like properties

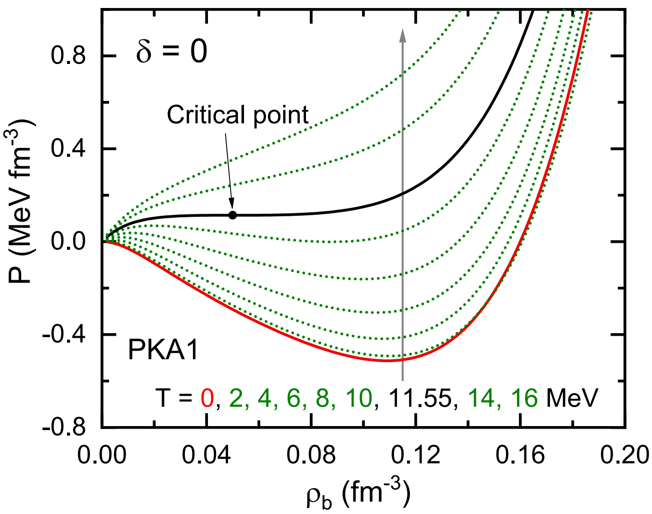

FIG. 1. Pressures P (MeV fm^{-3}) of symmetric nuclear matter ($\delta = 0$) as functions of nucleon density ρ_b (fm^{-3}) at various temperatures given by the RHF Lagrangian PKA1. In particular, the red (gray) and black solid lines represent the results at the temperature $T = 0$ and the critical temperature T_C, respectively.

of thermal nuclear matter described by PKA1 are rather different from the general CDFT calculations. In fact, a similar discrepancy can be also found in the LG phase diagram of asymmetric nuclear matter.

Figure 2 shows the LG phase diagrams of asymmetric nuclear matter at various temperatures, calculated by PKA1 [panel (a)] and PKO3 [panel (b)]. It can be seen that when the temperature T increases, the LG phase coexistent areas are gradually squeezed and disappear at the critical temperature T_C, namely the closer to T_C the more notably reduced the coexistent regions are, which is applicable for arbitrary RHF and RMF Lagrangians. Comparing the phase diagrams at the same temperature, it can be easily found that the LG phase coexistent areas predicted by PKA1 are systematically smaller than the ones predicted by PKO3, especially when approaching the T_C value given by PKA1, namely $T \geqslant 10$ MeV. In fact, similar situation is also found when comparing PKA1 and other relativistic Lagrangians. Combined with the results in Table I, it is evident that there exists a systematical difference between PKA1 and other relativistic Lagrangians in describing the LG phase transition of thermal nuclear matter.

TABLE I. Critical parameters of the LG phase transition of symmetric nuclear matter, i.e., the critical temperature T_C (MeV),the critical density ρ_C (fm^{-3}), the critical pressure P_C (MeV fm^{-3}), the critical incompressibility K_C (MeV), and the compressibility factor Z_C. The results are calculated by the RHF functionals with PKO3 [65] and PKA1 [64] and the RMF functionals with DD-ME2 [93] and PK1 [53].

	T_C	ρ_C	P_C	K_C	Z_C
PKA1	11.55	0.050	0.114	−40.69	0.196
PKO3	14.57	0.048	0.198	−75.03	0.286
DD-ME2	13.11	0.044	0.155	−62.92	0.267
PK1	15.11	0.049	0.223	−82.83	0.305

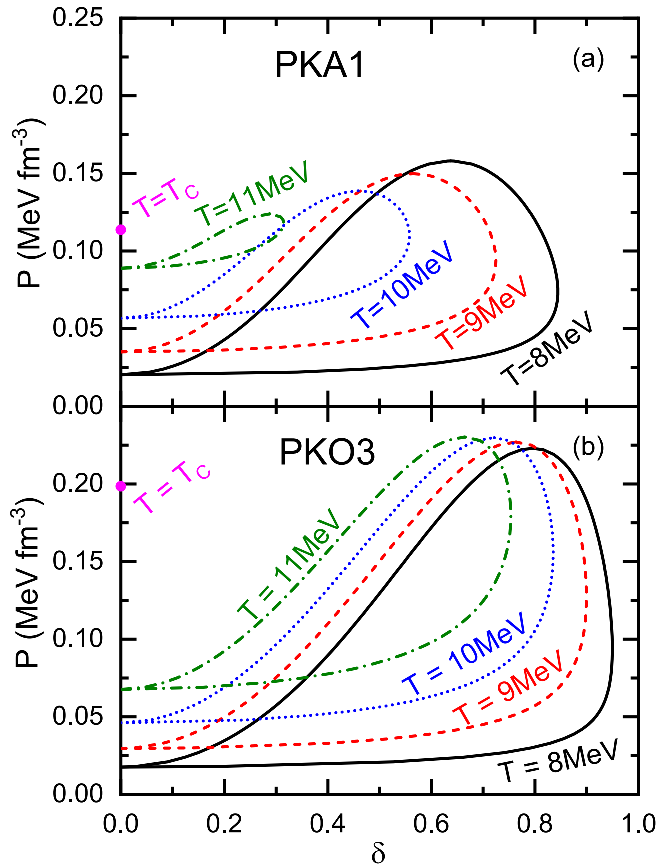

FIG. 2. LG phase diagrams of thermal nuclear matter at the temperatures $T = T_C$, 11, 10, 9, and 8 MeV, calculated by the RHF Lagrangians PKA1 (a) and PKO3 (b).

As pointed out in Ref. [81], the additional degree of freedom associated with the ρ-T coupling in PKA1 contributes a fairly strong attractive potential. It essentially changes the balance between the nuclear attraction and repulsion in nuclear systems, as well as the modeling of the in-medium effects of nuclear force. As a result, PKA1 improves systematically the description of the PSS restoration of the high-l PS partners in finite nuclei, referring to the available data [81]. Notice that the density range of the LG phase transition, particularly the LG phase coexistent area, is roughly coincident with the surface regions of finite nuclei, in which the density varies from a near saturated one to zero. Thus, the model deviations in describing the LG phase transition of thermal nuclear matter (see Table I and Fig. 2) can be related to the modeling of the in-medium balance between the nuclear attraction and repulsion [81], in which the role of the ρ-T coupling deserves further investigation.

B. Modeling of nuclear in-medium effects and LG phase transition of thermal nuclear matter

To clarify the role of the ρ-T coupling in describing the LG phase transition of thermal nuclear matter, we perform

TABLE II. Similar to Table I, but for the results given by the RHF Lagrangians PKA1 and PKO3 and the tests sets $x\kappa_\rho$.

	T_C	ρ_C	P_C	K_C	Z_C
PKA1	11.55	0.050	0.114	−40.69	0.196
$1.0\kappa_\rho$	13.58	0.038	0.151	−70.86	0.290
$0.9\kappa_\rho$	14.08	0.043	0.176	−73.02	0.288
$0.8\kappa_\rho$	14.67	0.048	0.206	−76.24	0.289
$0.7\kappa_\rho$	15.26	0.053	0.238	−80.29	0.292
PKO3	14.57	0.048	0.198	−75.03	0.286

a series of tests as illuminated by Ref. [81]. Starting from PKA1, we reduce the ρ-T coupling strength $\kappa_\rho = f_\rho(0)/g_\rho(0)$ by multiplying some factors $x = 1.0, 0.9, \ldots$, and the density dependence of the coupling strength $g_\omega(\rho_b)$ is replaced by that of $g_\sigma(\rho_b)$ to keep the density dependencies of $g_\sigma(\rho_b)$ and $g_\omega(\rho_b)$ paralleled. We found that such an operation may notably change the description of nuclear matter, especially the saturation mechanism. Thus, to provide a reasonable description of the saturation mechanism as much as possible, particularly keeping the binding energy E/A unchanged at the saturation density ρ_0, we further adjust the coupling strengths $g_\sigma(\rho_0)$ and $g_\omega(\rho_0)$ and the density-dependent parameters a_σ, b_σ, c_σ, and d_σ. The deduced parameter sets are denoted as $x\kappa_\rho$ ($x = 1.0$, 0.9, 0.8, and 0.7). With these tests, it can be helpful to understand the nuclear in-medium effects in the LG phase transition, which are found to be essential in restoring the PSS of the high-l PS partners [81]. It shall be remarked that the parametrizations $x\kappa_\rho$ are not fully performed, in which other parameters, except the mentioned ones, still remain unchanged. In the following, we mainly focus on the systematics from PKA1 to PKO3, a representative of other relativistic Lagrangians. Moreover, PKA1 and PKO3 have rather similar isovector ρ-V and π-PV couplings [81]. Thus, the testing parametrizations $x\kappa_\rho$ can be taken as the bridge between PKA1 and PKO3, which can help us to understand the effects of the in-medium balance between nuclear attraction and repulsion in determining the thermal equilibrium of nuclear matter [81].

Utilizing the sets $x\kappa_\rho$ ($x = 1.0$, 0.9, 0.8, and 0.7), we first performed the test calculations for symmetric thermal nuclear matter, especially focusing on the critical points. Table II shows the critical parameters given by the test sets $x\kappa_\rho$, in comparison with the original PKA1 and PKO3. It can be seen that from PKA1 to the set $1.0\kappa_\rho$, in which the ρ-T coupling strength κ_ρ remains unchanged and $g_\omega(\rho_b)$ shares the density dependence of the scalar coupling strength $g_\sigma(\rho_b)$, sudden changes are found on all the critical parameters. On the contrary, the values of all the selected critical quantities change smoothly along the $x\kappa_\rho$ series, approaching the predictions of the other relativistic Lagrangians, e.g., PKO3 that does not contain the ρ-T coupling.

Not only for the critical parameters of symmetric thermal nuclear matter, similar systematics can be also found in the LG phase diagrams. As an illustration, Fig. 3 shows the LG phase diagrams of thermal nuclear matter at the temperature $T = 10$ MeV, calculated by the RHF Lagrangians PKA1 and PKO3 and the sets $x\kappa_\rho$ ($x = 1.0$, 0.9, 0.8, and 0.7). Obviously, the phase coexistent areas are suddenly extended from PKA1 to the set $1.0\kappa_\rho$ with respect to both pressure and isospin asymmetry, when setting the coupling strength $g_\omega(\rho_b)$ to share the same density dependence as $g_\sigma(\rho_b)$ in the set $1.0\kappa_\rho$. Further reducing the ρ-T coupling strength κ_ρ, the phase diagrams are smoothly extended, and referring to the asymmetry δ the extension is less pronounced than referring to the pressure P. Eventually, the set $0.8\kappa_\rho$ presents a phase diagram rather similar to that of PKO3. Combining the results in Table II and Fig. 3, sudden changes from PKA1 to the set $1.0\kappa_\rho$ are found in both the critical parameters and the phase diagrams, and further reducing the ρ-T coupling strength κ_ρ the changes become smooth, leading to results similar to those of PKO3 by the set $0.8\kappa_\rho$.

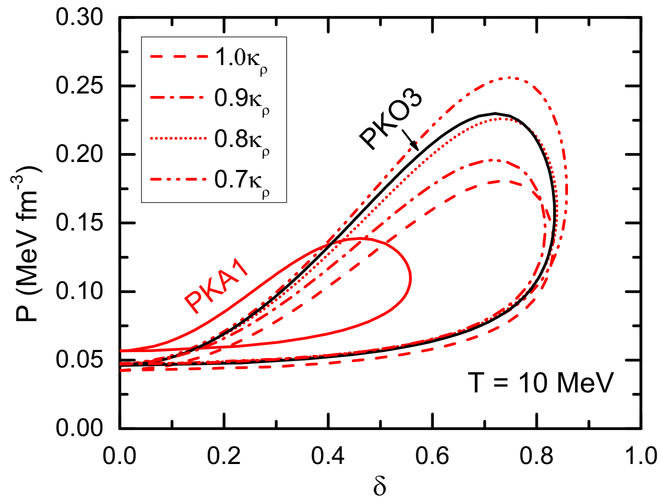

FIG. 3. LG phase diagrams of thermal nuclear matter at temperature $T = 10$ MeV given by the sets $x\kappa_\rho$ ($x = 1.0$, 0.9, 0.8, and 0.7), as compared to the ones given by the original RHF Lagrangians PKA1 and PKO3.

As mentioned in Ref. [81], the density-dependent behaviors of the isoscalar coupling strengths $g_\sigma(\rho_b)$ and $g_\omega(\rho_b)$ are nearly paralleled with each other for the popular DDRMF Lagrangians and the RHF ones PKOi ($i = 1$, 2, and 3), which are also predetermined for the test sets $x\kappa_\rho$. However, due to the strong ρ-T coupling that changes the in-medium balance between the nuclear attractions and repulsions [81], the density dependencies of $g_\sigma(\rho_b)$ and $g_\omega(\rho_b)$ in PKA1 are not paralleled any more. Similar to the systematics of the PSS restoration revealed in Ref. [81], the sudden changes happen from PKA1 to the set $1.0\kappa_\rho$, and the changes along the $x\kappa_\rho$ series are rather smooth (see both Table II and Fig. 3). Thus, the predicted van der Waals-like behaviors of thermal nuclear matter can be essentially related to the modeling of the nuclear in-medium effects, which manifest the notable model deviation between PKA1 and other relativistic Lagrangians.

As a reliability check of the testing sets $x\kappa_\rho$, Table III shows the bulk properties of nuclear matter at saturation densities obtained by the sets $x\kappa_\rho$, in comparison with the original PKA1 and PKO3. It can be seen that the saturation density ρ_0, as well as the symmetry energy J and the slope

TABLE III. Saturation properties of nuclear matter described by PKA1, PKO3, and the testing sets $x\kappa_\rho$ with $x = 1.0, 0.9, 0.8$, and 0.7, including the saturation density ρ_0 (fm^{-3}), the binding energy E/A (MeV), the symmetry energy J (MeV), the slope L (MeV), and the incompressibility K (MeV).

	ρ_0	E/A	J	K	L
PKA1	0.160	−15.83	36.02	229.96	103.00
$1.0\kappa_\rho$	0.134	−15.83	28.93	225.21	69.81
$0.9\kappa_\rho$	0.140	−15.83	30.14	258.70	76.88
$0.8\kappa_\rho$	0.146	−15.83	31.28	292.04	83.38
$0.7\kappa_\rho$	0.150	−15.83	32.26	324.09	89.43
PKO3	0.153	−16.04	33.09	264.98	83.47

L, is notably reduced from PKA1 to the set $1.0\kappa_\rho$, in which the coupling strengths $g_\sigma(\rho_b)$ and $g_\omega(\rho_b)$ are fixed to share the same density dependence. While further reducing the ρ-T coupling strength, namely from $1.0\kappa_\rho$ to $0.7\kappa_\rho$, the values of ρ_0, J, and L are smoothly enlarged, approaching the values given by PKO3. In contrast to that, the incompressibility K, e.g., the ones given by the sets $0.8\kappa_\rho$ and $0.7\kappa_\rho$, tends to beyond the one of PKO3, which limits the further reduction of κ_ρ. Such limitation is due to the rigid requirement of the same density dependence of $g_\sigma(\rho_b)$ and $g_\omega(\rho_b)$, which may also account for the relatively small ρ_0 value given by the set $1.0\kappa_\rho$ in Table III. Even though, it can be seen from Table II and Fig. 3 that there is no significant difference between the results given by the set $0.8\kappa_\rho$ and PKO3, from which one can understand the role played by the nuclear in-medium effects in describing the properties of the LG phase transition of thermal nuclear matter.

To better understand the systematics from PKA1 to the $x\kappa_\rho$ series and further to the popular relativistic Lagrangians, we show in Fig. 4 the correlations between the critical parameters T_C and P_C [panel (a)] and the correlations between T_C and K_C [panel (b)]. The results are extracted from the calculations with 20 selected relativistic Lagrangians in Ref. [33], PKA1, and the test sets $x\kappa_\rho$ ($x = 1.0, 0.9, 0.8$, and 0.7). As an additional illustration, we also present the results given by another series of testing parametrizations $x\kappa_\rho^*$ ($x = 0.9$, 0.8, and 0.7), in which the ρ-T coupling strength is similarly reduced and the density dependencies of $g_\omega(\rho_b)$ and $g_\sigma(\rho_b)$ remain unchanged from PKA1. Similar to the sets $x\kappa_\rho$, the binding energy E/A at saturation density is also fixed as the one given by PKA1, and the coupling strengths $g_\omega(\rho_0)$ and $g_\sigma(\rho_0)$ are adjusted to get a reasonable description of the saturation mechanism as much as possible in deducing the sets $x\kappa_\rho^*$. In contrast to the sets $x\kappa_\rho$, the calculations show that the values of ρ_0, J, L, and K given by the sets $x\kappa_\rho^*$, which are not shown for simplicity, are all enlarged from the original PKA1 and monotonously increase with the reduction of the ρ-T coupling strength, showing remarkable deviations from the values given by the popular RMF and RHF models.

As shown in Fig. 4, from PKA1 to the $x\kappa_\rho$ series, in which the isoscalar coupling strengths $g_\sigma(\rho_b)$ and $g_\omega(\rho_b)$ are set to share the same density dependence, the results given by the set $1.0\kappa_\rho$ become suddenly neighboring to the other RHF and RMF Lagrangians. Besides, as seen from Fig. 4, nice linear correlations are preserved along the $x\kappa_\rho$ series from $x = 1.0$ to 0.7, being coincident with the selected RHF and RMF Lagrangians. In particular from PKA1 to the set $1.0\kappa_\rho$, the critical temperature T_C increases greatly, about 2.0 MeV (see Table II), which becomes farther away from the selected temperature $T = 10$ MeV in Fig. 3. Following the systematics indicated by Fig. 2, it is not difficult to understand the largely extended LG phase diagrams in Fig. 3 from the original PKA1 to the set $1.0\kappa_\rho$. As we mentioned, the density dependencies of $g_\sigma(\rho_b)$ and $g_\omega(\rho_b)$ are nearly paralleled with each another, i.e., $g_\sigma(\rho_b)/g_\omega(\rho_b) \approx C$, for the popular DDRMF Lagrangians and the DDRHF ones PKOi ($i = 1$, 2, and 3), but not for PKA1 because of the ρ-T coupling. In contrast to the testing sets $x\kappa_\rho$, the density dependencies of $g_\sigma(\rho_b)$ and $g_\omega(\rho_b)$ for other testing sets $x\kappa_\rho^*$ are not changed from PKA1, and nice linear correlations are found along PKA1 to the sets $x\kappa_\rho^*$ but notably deviate from the other RMF and RHF Lagrangians. Thus, as indicated by the coincident systematics from Table II and Figs. 3 and 4, it can be concluded that the residual nuclear in-medium effects, deduced from the unparalleled density dependencies of $g_\sigma(\rho_b)$ and $g_\omega(\rho_b)$, play an essential role in determining the van der Waals-like behavior of thermal nuclear matter.

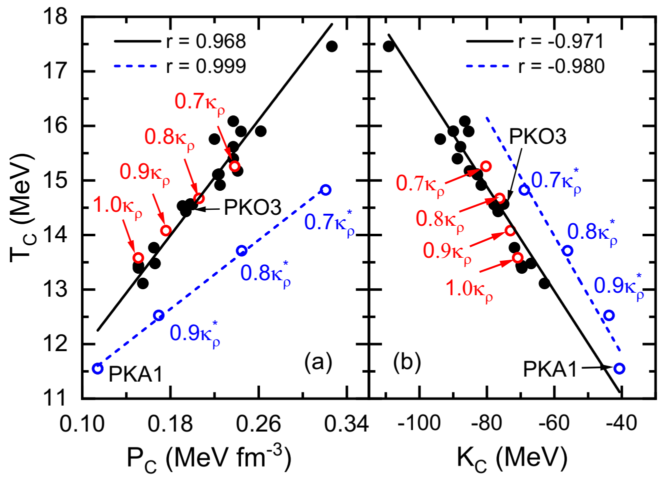

FIG. 4. Plots (a) and (b) show the correlation between the critical parameters T_C (MeV) and P_C (MeV fm^{-3}) and the correlation between T_C (MeV) and K_C (MeV), respectively. The solid circles correspond to 20 selected relativistic Lagrangians from Ref. [33] and PKA1, and the open circles correspond to the testing sets $x\kappa_\rho$ with $x = 1.0$ to 0.7 (in red) and $x\kappa_\rho^*$ with $x = 0.9$, 0.8, and 0.7 (in blue). As the references, the solid and dashed lines represent the linear fittings with the Pearson correlation coefficient r.

IV. SUMMARY

In this work, the liquid-gas (LG) phase transition of thermal nuclear matter is studied by using the relativistic Hartree-Fock (RHF) Lagrangian PKA1, and particular efforts are devoted to the effects of the in-medium balance between nuclear attraction and repulsion in determining the thermal equilibrium of nuclear matter. It is found that PKA1 predicts rather different critical properties of the LG phase transition for symmetric nuclear matter and notably squeezed phase diagrams for asymmetric nuclear matter, as compared to the popular relativistic mean-field (RMF) models and the RHF ones PKO*i* ($i = 1$, 2, and 3), in which the density dependencies of the isoscalar coupling strengths $g_\sigma(\rho_b)$ and $g_\omega(\rho_b)$ are nearly paralleled in contrast to PKA1.

Aiming at such notable model deviations, a series of testing parametrizations $x\kappa_\rho$ based on PKA1 is proposed by setting the same density dependencies for $g_\sigma(\rho_b)$ and $g_\omega(\rho_b)$ and rescaling the ρ-tensor coupling strength κ_ρ with the factor $x \leqslant 1.0$. Sudden changes of both critical parameters and LG phase diagrams are found from PKA1 to the $x\kappa_\rho$ series, which eventually present results similar to those of PKO3 with $x = 0.8$. Further, combined with the results given by another testing parametrization $x\kappa_\rho^*$, in which the density dependencies of $g_\sigma(\rho_b)$ and $g_\omega(\rho_b)$ remain unchanged from PKA1 and κ_ρ is similarly reduced, it is illustrated that the van der Waals-like behavior of thermal nuclear matter is essentially related to the in-medium balance between nuclear attraction and repulsion, which corresponds to various modeling of the nuclear in-medium effects, and the residual nuclear in-medium effects which originate from the unparalleled density dependencies of $g_\sigma(\rho_b)$ and $g_\omega(\rho_b)$ play the key role.

Our results not only reveal the significance of nuclear in-medium effects in determining the thermal equilibrium of nuclear matter that is meaningful for the cooling process of neutron stars but also pave a way to model the in-medium nuclear force from the aspect of thermal statistics of nuclear systems, such as the critical temperature deduced from future delicate experiments, such as heavy-ion collisions.

ACKNOWLEDGMENTS

This work was partly supported by the Natural Science Foundation of China under Grants No. 11675065 and No. 11875152 and by the Strategic Priority Research Program of Chinese Academy of Sciences under Grant No. XDB34000000.

S.Y. and X.D.S. contributed equally to this paper.

[1] P. J. Siemens, Nature (London) **305**, 410 (1983).
[2] V. Vovchenko, D. V. Anchishkin, and M. I. Gorenstein, Phys. Rev. C **91**, 064314 (2015).
[3] J. E. Finn, S. Agarwal, A. Bujak, J. Chuang, L. J. Gutay, A. S. Hirsch, R. W. Minich, N. T. Porile, R. P. Scharenberg, B. C. Stringfellow *et al.*, Phys. Rev. Lett. **49**, 1321 (1982).
[4] A. D. Panagiotou, M. W. Curtin, H. Toki, D. K. Scott, and P. J. Siemens, Phys. Rev. Lett. **52**, 496 (1984).
[5] J. B. Natowitz, K. Hagel, Y. Ma, M. Murray, L. Qin, R. Wada, and J. Wang, Phys. Rev. Lett. **89**, 212701 (2002).
[6] F. Gobet, B. Farizon, M. Farizon, M. J. Gaillard, J. P. Buchet, M. Carré, P. Scheier, and T. D. Märk, Phys. Rev. Lett. **89**, 183403 (2002).
[7] A. Le Fèvre, G. Auger, M. L. Begemann-Blaich, N. Bellaize, R. Bittiger, F. Bocage, B. Borderie, R. Bougault, B. Bouriquet, J. L. Charvet *et al.* (INDRA and ALADIN Collaborations), Phys. Rev. Lett. **94**, 162701 (2005).
[8] C. Sfienti, P. Adrich, T. Aumann, C. O. Bacri, T. Barczyk, R. Bassini, S. Bianchin, C. Boiano, A. S. Botvina, A. Boudard *et al.* (ALADIN2000 Collaboration), Phys. Rev. Lett. **102**, 152701 (2009).
[9] J. B. Elliott, P. T. Lake, L. G. Moretto, and L. Phair, Phys. Rev. C **87**, 054622 (2013).
[10] H. R. Jaqaman, A. Z. Mekjian, and L. Zamick, Phys. Rev. C **29**, 2067 (1984).
[11] A. L. Goodman, J. I. Kapusta, and A. Z. Mekjian, Phys. Rev. C **30**, 851 (1984).
[12] R. K. Su, S. D. Yang, and T. T. S. Kuo, Phys. Rev. C **35**, 1539 (1987).
[13] H. Müller and B. D. Serot, Phys. Rev. C **52**, 2072 (1995).
[14] M. Baldo and L. S. Ferreira, Phys. Rev. C **59**, 682 (1999).
[15] Y. G. Ma, Phys. Rev. Lett. **83**, 3617 (1999).
[16] V. A. Karnaukhov, H. Oeschler, S. P. Avdeyev, E. V. Duginova, V. K. Rodionov, A. Budzanowski, W. Karcz, O. V. Bochkarev, E. A. Kuzmin, L. V. Chulkov *et al.*, Phys. Rev. C **67**, 011601(R) (2003).
[17] P. Chomaz, M. Colonna, and J. Randrup, Phys. Rep. **389**, 263 (2004).
[18] C. Das, S. D. Gupta, W. Lynch, A. Mekjian, and M. Tsang, Phys. Rep. **406**, 1 (2005).
[19] M. Pichon, B. Tamain, R. Bougault, F. Gulminelli, O. Lopez, E. Bonnet, B. Borderie, A. Chbihi, R. Dayras, J. Frankland *et al.*, Nucl. Phys. A **779**, 267 (2006).
[20] G. E. Brown, J. W. Holt, C. H. Lee, and M. Rho, Phys. Rep. **439**, 161 (2007).
[21] B. A. Li, L. W. Chen, and C. M. Ko, Phys. Rep. **464**, 113 (2008).
[22] B. Borderie and J. Frankland, Prog. Part. Nucl. Phys. **105**, 82 (2019).
[23] C. J. Pethick, Rev. Mod. Phys. **64**, 1133 (1992).
[24] M. Prakash, I. Bombaci, M. Prakash, P. J. Ellis, J. M. Lattimer, and R. Knorren, Phys. Rep. **280**, 1 (1997).
[25] J. M. Lattimer and M. Prakash, Science **304**, 536 (2004).
[26] J. M. Lattimer and M. Prakash, Phys. Rep. **621**, 127 (2016).
[27] M. A. Aloy, J. M. Ibáñez, N. Sanchis-Gual, M. Obergaulinger, J. A. Font, S. Serna, and A. Marquina, Mon. Not. Roy. Astron. Soc. **484**, 4980 (2019).
[28] W. Zuo, Z. H. Li, A. Li, and G. C. Lu, Phys. Rev. C **69**, 064001 (2004).
[29] A. Rios, A. Polls, A. Ramos, and H. Müther, Phys. Rev. C **78**, 044314 (2008).
[30] J. Xu, L. W. Chen, B. A. Li, and H. R. Ma, Phys. Lett. B **650**, 348 (2007).
[31] A. Rios, Nucl. Phys. A **845**, 58 (2010).
[32] V. Vovchenko, Phys. Rev. C **96**, 015206 (2017).
[33] S. Yang, B. N. Zhang, and B. Y. Sun, Phys. Rev. C **100**, 054314 (2019).
[34] A. McIntosh, A. Bonasera, P. Cammarata, K. Hagel, L. Heilborn, Z. Kohley, J. Mabiala, L. May, P. Marini, A. Raphelt *et al.*, Phys. Lett. B **719**, 337 (2013).
[35] A. B. McIntosh, A. Bonasera, Z. Kohley, P. J. Cammarata, K. Hagel, L. Heilborn, J. Mabiala, L. W. May, P. Marini, A. Raphelt *et al.*, Phys. Rev. C **87**, 034617 (2013).

[36] M. Dutra, O. Lourenço, A. Delfino, J. S. Sa Martins, C. Providência, S. S. Avancini, and D. P. Menezes, Phys. Rev. C **77**, 035201 (2008).
[37] B. K. Sharma and S. Pal, Phys. Rev. C **81**, 064304 (2010).
[38] G. H. Zhang and W. Z. Jiang, Phys. Lett. B **720**, 148 (2013).
[39] A. Fedoseew and H. Lenske, Phys. Rev. C **91**, 034307 (2015).
[40] R. V. Poberezhnyuk, V. Vovchenko, M. I. Gorenstein, and H. Stoecker, Phys. Rev. C **99**, 024907 (2019).
[41] B. K. Sharma and S. Pal, Phys. Rev. C **82**, 055802 (2010).
[42] B. D. Serot and J. D. Walecka, The relativistic nuclear many-body problem, in *Advances in Nuclear Physics*, Vol.16, edited by J. W. Negele and E. Vogte (Plenum, New York, 1986).
[43] P. G. Reinhard, Rep. Prog. Phys. **52**, 439 (1989).
[44] P. Ring, Prog. Part. Nucl. Phys. **37**, 193 (1996).
[45] M. Bender and P. H. Heenen, Rev. Mod. Phys. **75**, 121 (2003).
[46] D. Vretenar, A. V. Afanasjev, G. A. Lalazissis, and P. Ring, Phys. Rep. **409**, 101 (2005).
[47] J. Meng, H. Toki, S. Zhou, S. Zhang, W. Long, and L. Geng, Prog. Part. Nucl. Phys. **57**, 470 (2006).
[48] T. Nikšić, D. Vretenar, and P. Ring, Prog. Part. Nucl. Phys. **66**, 519 (2011).
[49] J. Meng and S. G. Zhou, J. Phys. G: Nucl. Part. Phys. **42**, 093101 (2015).
[50] J. Meng, *Relativistic Density Functional for Nuclear Structure*, International Review of Nuclear Physics, Vol. 10 (World Scientific, Singapore, 2016).
[51] J. Boguta and A. Bodmer, Nucl. Phys. A **292**, 413 (1977).
[52] Y. Sugahara and H. Toki, Nucl. Phys. A **579**, 557 (1994).
[53] W. Long, J. Meng, N. Van Giai, and S. G. Zhou, Phys. Rev. C **69**, 034319 (2004).
[54] R. Brockmann and H. Toki, Phys. Rev. Lett. **68**, 3408 (1992).
[55] H. Lenske and C. Fuchs, Phys. Lett. B **345**, 355 (1995).
[56] C. Fuchs, H. Lenske, and H. H. Wolter, Phys. Rev. C **52**, 3043 (1995).
[57] S. Typel and H. Wolter, Nucl. Phys. A **656**, 331 (1999).
[58] O. Lourenço, M. Dutra, and D. P. Menezes, Phys. Rev. C **95**, 065212 (2017).
[59] A. Bouyssy, S. Marcos, J. F. Mathiot, and N. Van Giai, Phys. Rev. Lett. **55**, 1731 (1985).
[60] A. Bouyssy, J. F. Mathiot, N. Van Giai, and S. Marcos, Phys. Rev. C **36**, 380 (1987).
[61] P. Bernardos, V. N. Fomenko, N. V. Giai, M. L. Quelle, S. Marcos, R. Niembro, and L. N. Savushkin, Phys. Rev. C **48**, 2665 (1993).
[62] S. Marcos, L. N. Savushkin, V. N. Fomenko, M. López-Quelle, and R. Niembro, J. Phys. G: Nucl. Part. Phys. **30**, 703 (2004).
[63] W. H. Long, N. V. Giai, and J. Meng, Phys. Lett. B **640**, 150 (2006).
[64] W. H. Long, H. Sagawa, N. V. Giai, and J. Meng, Phys. Rev. C **76**, 034314 (2007).
[65] W. H. Long, H. Sagawa, J. Meng, and N. V. Giai, EuroPhys. Lett. **82**, 12001 (2008).
[66] W. H. Long, P. Ring, J. Meng, N. Van Giai, and C. A. Bertulani, Phys. Rev. C **81**, 031302(R) (2010).
[67] H. Liang, N. Van Giai, and J. Meng, Phys. Rev. Lett. **101**, 122502 (2008).
[68] H. Z. Liang, N. V. Giai, and J. Meng, Phys. Rev. C **79**, 064316 (2009).
[69] W. H. Long, T. Nakatsukasa, H. Sagawa, J. Meng, H. Nakada, and Y. Zhang, Phys. Lett. B **680**, 428 (2009).
[70] Z. M. Niu, Y. F. Niu, H. Z. Liang, W. H. Long, T. Nikšić, D. Vretenar, and J. Meng, Phys. Lett. B **723**, 172 (2013).
[71] L. J. Wang, J. M. Dong, and W. H. Long, Phys. Rev. C **87**, 047301 (2013).
[72] J. J. Li, W. H. Long, J. Margueron, and N. V. Giai, Phys. Lett. B **732**, 169 (2014).
[73] J. J. Li, J. Margueron, W. H. Long, and N. V. Giai, Phys. Lett. B **753**, 97 (2016).
[74] L. J. Jiang, S. Yang, J. M. Dong, and W. H. Long, Phys. Rev. C **91**, 025802 (2015).
[75] L. J. Jiang, S. Yang, B. Y. Sun, W. H. Long, and H. Q. Gu, Phys. Rev. C **91**, 034326 (2015).
[76] Z. Wang, Q. Zhao, H. Liang, and W. H. Long, Phys. Rev. C **98**, 034313 (2018).
[77] B. Y. Sun, W. H. Long, J. Meng, and U. Lombardo, Phys. Rev. C **78**, 065805 (2008).
[78] W. H. Long, B. Y. Sun, K. Hagino, and H. Sagawa, Phys. Rev. C **85**, 025806 (2012).
[79] Q. Zhao, B. Y. Sun, and W. H. Long, J. Phys. G: Nucl. Part. Phys. **42**, 095101 (2015).
[80] Z. W. Liu, Z. Qian, R. Y. Xing, J. R. Niu, and B. Y. Sun, Phys. Rev. C **97**, 025801 (2018).
[81] J. Geng, J. J. Li, W. H. Long, Y. F. Niu, and S. Y. Chang, Phys. Rev. C **100**, 051301(R) (2019).
[82] A. Arima, M. Harvey, and K. Shimizu, Phys. Lett. B **30**, 517 (1969).
[83] K. T. Hecht and A. Adler, Nucl. Phys. A **137**, 129 (1969).
[84] J. N. Ginocchio, Phys. Rev. Lett. **78**, 436 (1997).
[85] J. Meng, K. Sugawara-Tanabe, S. Yamaji, P. Ring, and A. Arima, Phys. Rev. C **58**, R628 (1998).
[86] J. Meng, K. Sugawara-Tanabe, S. Yamaji, and A. Arima, Phys. Rev. C **59**, 154 (1999).
[87] W. H. Long, H. Sagawa, J. Meng, and N. V. Giai, Phys. Lett. B **639**, 242 (2006).
[88] H. Z. Liang, J. Meng, and S.-G. Zhou, Phys. Rep. **570**, 1 (2015).
[89] L. S. Geng, J. Meng, T. Hiroshi, W. H. Long, and G. Shen, Chin. Phys. Lett. **23**, 1139 (2006).
[90] M. J. D. Powell, A hybrid method for nonlinear equations, in *Numerical Methods for Nonlinear Algebraic Equations*, edited by P. Rabinowitz (Gorden and Breach, London, 1970).
[91] J. Silva, O. Lourenço, A. Delfino, J. S. Martins, and M. Dutra, Phys. Lett. B **664**, 246 (2008).
[92] O. Lourenço, B. M. Santos, M. Dutra, and A. Delfino, Phys. Rev. C **94**, 045207 (2016).
[93] G. A. Lalazissis, T. Nikšić, D. Vretenar, and P. Ring, Phys. Rev. C **71**, 024312 (2005).